

COMPARISON BETWEEN HPM AND FINITE FOURIER SOLUTION IN STATIC ANALYSIS OF FGPM BEAM UNDER THERMAL LOAD

AHAD ARMIN

*Amirkabir University of Technology, Department of Mechanical Engineering, Tehran, Iran
e-mail: aarmin84@gmail.com; ahad_armin_mec84@yahoo.com*

IMAN SHAFIEENEJAD

*K.N. Toosi University of Technology, Department of Aerospace Engineering, Tehran, Iran
e-mail: shafiee_iman@yahoo.com*

NIMA MOALLEMI

*Iran University of Science and Technology, Department of Mechanical Engineering, Tehran, Iran
e-mail: nima.moallemi@yahoo.com*

ALIREZA B. NOVINZADEH

*K.N. Toosi University of Technology, Department of Aerospace Engineering, Tehran, Iran
e-mail: novinzadeh@kntu.ac.ir*

Linear and nonlinear phenomena play important role in applied mathematics, physics and also in engineering problems in which any parameter may vary depending on different factors. In recent years, the homotopy perturbation method (HPM) is constantly being developed and applied to solve various linear and nonlinear problems. In this paper, static analysis of functionally graded piezoelectric beams based on the first-order shear deformation theory under thermal loads has been investigated. The beam with a functionally graded piezoelectric material (FGPM) is graded in the thickness direction and a simple power law index governs the piezoelectric material properties. The electric potential is assumed linear across the beam thickness. The governing equations are obtained using potential energy and Hamilton's principle and may lead to a system of differential equations. We suggest two methods to solve this problem, the homotopy perturbation and analytical solution obtained by the finite Fourier transformation. The homotopy perturbation method and a proper algorithm are suggested to solve simultaneous differential equations. The results are presented for different power law indexes under uniform thermal gradient. The results are compared with the analytical solution obtained by the finite Fourier transformation for simply supported boundary conditions.

Key words: functionally graded piezoelectric material, thermal load, first-order shear deformation theory, homotopy perturbation method

1. Introduction

Since the piezoelectric phenomenon was first discovered, which is widely used to manufacture smart structures, various piezoelectric sensors, actuators, conductors and transducers are implemented to operate in structural design problems. Piezoelectric actuators and sensors have novel applications for microelectromechanical systems and smart material systems, especially in the medical and aerospace industries (Chen *et al.*, 2004; Takagi *et al.*, 2003). Since most aerospace applications involve operations in changing thermal environments, increased interests in piezothermoelasticity during recent years have addressed the thermo- and electromechanical behaviour of such materials. Nowadays, the use of functionally graded materials (FGM) has gained intensive attention especially in extreme high temperature environments and reduction high thermal stresses. FGMs are inhomogeneous materials the material properties of which vary continuously in one (or more) direction(s). This is achieved usually by gradually changing the composition of constituent materials along the thickness to obtain smooth variation of material properties and optimum responses to externally applied thermo-mechanical loadings. FGMs are now developed for the general use as structural components in high temperature environments and being strongly considered as potential structural material candidates for future high-speed spacecraft. Typical FGMs are made of a mixture of ceramic and metal, or a combination of different metals or different ceramics that are appropriate to achieve the desired objective. Another kind of FGMs, called functionally graded piezoelectric materials (FGPM), obtained even more attention in the recent years (Wu *et al.*, 2002).

It is well known that piezoelectric materials have been widely used as sensors and actuators in control systems. Smart structures or elements made of these so-called FGPMs are usually superior to conventional sensors and actuators and are often made of the uni-morph, bi-morph and multimorph materials. For a piezoelectric laminate with homogeneous material properties in layers, large bending displacements, high stress concentrations, creep at high temperature and failure from interfacial bonding are usually presented at the layer interfaces under a mechanical or electric loading. These effects may lead to lifetime limitations and reliability reduction. To reduce the drawbacks, piezoelectric materials and structures with functionally graded material properties along the layer-thickness direction have been introduced and fabricated. The additional advantage of FGPM actuators is that no bonding agent is needed to bond the piezoelectric ceramic plates, because the piezoelectric layers and the inner electrode can be formed together by the sintering process.

The functionally graded sensors and actuators play an important role in the field of micro structural engineering (Pin *et al.*, 2006; Liao, 1995).

This paper presents static analysis of an FGPM beam based on the first-order shear deformation theory under thermal load. The analysis is based on the homotopy perturbation method (HPM) proposed by Liao (1995, 1997). The results are compared with the finite Fourier transformation for different power law indexes. Using this method, one concludes that it is a proper method to overcome FGPM's difficulties in engineering problems.

2. Derivation of governing equations

Consider a functionally graded piezoelectric beam as shown in Fig. 1. The material properties change functionally between the upper and lower surfaces across the beam thickness.

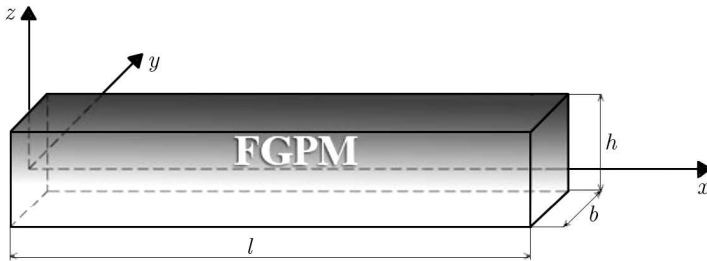


Fig. 1. FGPM beam and coordinates

In the model that is used in this paper, the material properties are expressed as

$$P(z) = P_{ul} \left(\frac{2z+h}{2h} \right)^n + P_l \quad P_{ul} = P_u - P_l \quad (2.1)$$

where z is coordinate along the thickness direction of the beam, P_u , P_l are properties of the upper surface and the lower surface, respectively; and h is the thickness of the FGPM beam. The power n is the volume fraction exponent.

FGPMs are particularly effective in high-temperature environments. In the present analysis, constant surface temperatures are imposed at the upper and lower surfaces. The variation in temperature is assumed to occur along the thickness direction only. Thus, the steady-state heat transfer equation is reduced to a one-dimensional equation as

$$-\frac{d}{dz} \left(K(z) \frac{dT}{dz} \right) = 0 \quad (2.2)$$

with boundary conditions such that $T = T_u$ at $z = h/2$ and $T = T_l$ at $z = -h/2$. Here, T is the temperature; T_u and T_l are the applied temperatures on the upper and lower surfaces, respectively; z is the coordinate in the thickness direction and K is the thermal conductivity which varies according to the profile given by Eq. (2.2). The solution to Eq. (2.3) can be obtained by means of the polynomial series (Lanhe *et al.*, 2007)

$$T(z) = T_l + \frac{\Delta T}{\Lambda} \left[\frac{2z+h}{2h} + \sum_{i=1} \frac{(-1)^i K_{ul}^i}{(ni+1)K_l^i} \left(\frac{2z+h}{2h} \right)^{ni+1} \right] \quad (2.3)$$

with

$$\Lambda = 1 + \sum_{i=1} \frac{(-1)^i K_{ul}^i}{(ni+1)K_l^i} \quad (2.4)$$

Using the first-order shear deformation theory, the displacement components are

$$u(x, z) = u_0(x) - z\psi(x) \quad w(x) = w_0(x) \quad (2.5)$$

where u is the axial displacement, w is the transverse displacement in the z direction and ψ is the rotation angle of the cross-section with respect to the longitudinal axis. The subscript zero denotes the middle surface displacement. In terms of the displacement components, the normal and shear strains are given by

$$\varepsilon_x = u_{0,x} - z\psi_{,x} \quad \gamma_{xz} = w_{0,x} - \psi \quad (2.6)$$

where the comma in subscript denotes partial differentiation.

The constitutive relationships describing electrical and mechanical interactions for piezoelectric materials are given as (Wang and Noda, 2001)

$$\sigma_{ij} = c_{ijkl}\varepsilon_{kl} - e_{lij}E_l - \beta_{ij}\theta \quad D_i = e_{ikl}\varepsilon_{kl} + \eta_{il}E_l + p_i\theta \quad (2.7)$$

here, σ_{ij} and ε_{kl} are the stress and strain tensors, respectively, D_i is the electrical displacement vector, $E_l = -\varphi_{,l}$ is the electrical field vector and φ is the electrical potential, c_{ijkl} is the elasticity matrix, e_{ikl} - piezoelectric constant matrix, η_{il} - dielectric permittivity coefficient matrix, $\beta_{ij} = c_{ijkl}\alpha_{kl}$ with α_{kl} being the thermal expansion coefficients, p_i denotes the pyroelectric constants and $\theta = T - T_0$, where T_0 is the reference temperature.

For an FGPM beam with a small width, assume the plane state of stress ($\sigma_y = \sigma_{yz} = \sigma_{xy} = 0$), neglect the transverse normal stress ($\sigma_z \approx 0$) and assume the axial and transverse displacements u , w and the electric potential φ to be independent of y . The electric field E_x is considered non-zero, as it may be induced by the piezoelectric coupling. With these assumptions, the general

linear constitutive equations for the stresses and the electric displacements reduce to (Kapuria *et al.*, 2004)

$$\begin{aligned}
 \sigma_x &= \widehat{E}(z)\varepsilon_x - e_{31}(z)E_z - \widehat{E}(z)\alpha(z)\theta = \widehat{E}(z)(u_{0,x} - z\psi_{,x}) + e_{31}(z)\varphi_{,z} + \\
 &\quad - \widehat{E}(z)\alpha(z)\theta \\
 \sigma_{xz} &= \widehat{G}(z)\gamma_{xz} - e_{15}(z)E_x = \widehat{G}(z)(w_{0,x} - \psi) + e_{15}(z)\varphi_{,x} \\
 D_x &= e_{15}(z)\gamma_{xz} + \eta_{11}(z)E_x = e_{15}(z)(w_{0,x} - \psi) - \eta_{11}(z)\varphi_{,x} \\
 D_z &= e_{31}(z)\varepsilon_x + \eta_{33}(z)E_z + p_3(z)\theta = e_{31}(z)(u_{0,x} - z\psi_{,x}) - \eta_{33}(z)\varphi_{,z} + \\
 &\quad + p_3(z)\theta
 \end{aligned} \tag{2.8}$$

where \widehat{E} and \widehat{G} are Young's modulus and shear modulus, respectively. For mathematical simplification, the potential φ is assumed linear across the FGPM beam thickness as (Trindade and Benjeddou, 2006)

$$\varphi(x, z) = \frac{z}{h}[\varphi^+(x) - \varphi^-(x)] + \frac{1}{2}[\varphi^+(x) + \varphi^-(x)] \tag{2.9}$$

where φ^+ and φ^- are the electric potentials on the upper and lower surfaces of the FGPM beam, respectively.

For static analysis of the beam, the variational formulation may be written using the virtual work principle extended to piezoelectric media (Kapuria *et al.*, 2004)

$$\delta W - \delta H = 0 \tag{2.10}$$

where δH and δW are the virtual works of electromechanical internal and applied mechanical forces, respectively. The virtual work done by the electromechanical internal forces in the FGPM beam is

$$\delta H = \int_v (\sigma_x \delta \varepsilon_x + \sigma_{xz} \delta \gamma_{xz} - D_x \delta E_x - D_z \delta E_z) dv \tag{2.11}$$

Using constitutive relations Eq. (2.7) for the strain tensor, Eqs. (2.8) and the electric field relations of Eq. (2.9), and substituting into Eq. (2.11) and carrying the variational formulation, the governing equations are obtained as

$$\begin{aligned}
 \delta u_0 &: A'_1 u_{0,xx} + A'_2 \psi_{,xx} + A'_3 \varphi_{,x}^+ + A'_4 \varphi_{,x}^- = 0 \\
 \delta \psi &: B'_1 u_{0,xx} + B'_2 \psi + B'_3 \psi_{,xx} + B'_4 w_{0,x} + B'_5 \varphi_{,x}^+ + B'_6 \varphi_{,x}^- = 0 \\
 \delta w_0 &: C'_1 \psi_{,x} + C'_2 w_{0,xx} + C'_3 \varphi_{,xx}^+ + C'_4 \varphi_{,xx}^- = 0 \\
 \delta \varphi^+ &: D'_1 u_{0,x} + D'_2 \psi_{,x} + D'_3 w_{0,xx} + D'_4 \varphi^+ + D'_5 \varphi^- + D'_6 \varphi_{,xx}^+ + D'_7 \varphi_{,xx}^- = D'_8 \\
 \delta \varphi^- &: E'_1 u_{0,x} + E'_2 \psi_{,x} + E'_3 w_{0,xx} + E'_4 \varphi^+ + E'_5 \varphi^- + E'_6 \varphi_{,xx}^+ + E'_7 \varphi_{,xx}^- = E'_8
 \end{aligned} \tag{2.12}$$

where A' , B' , C' , D' , and E' are given in Appendix A.

3. Solution procedure

To solve the simultaneous governing equations, dimensionless values are defined as

$$\begin{aligned} \bar{u}_0 &= \frac{u_0}{l} & \bar{w}_0 &= \frac{w_0}{l} & \bar{x} &= \frac{x}{l} \\ \bar{\varphi}^+ &= \frac{e_{31u}}{\hat{E}_u l} \varphi^+ & \bar{\varphi}^- &= \frac{e_{31u}}{\hat{E}_u l} \varphi^- \end{aligned} \quad (3.1)$$

where l is the length of the beam, \hat{E}_u and e_{31u} are Young's modulus and piezoelectric constant of the upper surface of the FGPM beam, respectively. The sign $(-)$ indicates the dimensionless value.

Using the dimensionless parameters, governing Eqs. (2.12) are given as

$$\begin{aligned} a'_1 \bar{u}_{0,\bar{x}\bar{x}} + a'_2 \bar{\psi}_{,\bar{x}\bar{x}} + a'_3 \bar{\varphi}_{,\bar{x}}^+ + a'_4 \bar{\varphi}_{,\bar{x}}^- &= 0 \\ b'_1 \bar{u}_{0,\bar{x}\bar{x}} + b'_2 \bar{\psi} + b'_3 \bar{\psi}_{,\bar{x}\bar{x}} + b'_4 \bar{w}_{0,\bar{x}} + b'_5 \bar{\varphi}_{,\bar{x}}^+ + b'_6 \bar{\varphi}_{,\bar{x}}^- &= 0 \\ c'_1 \bar{\psi}_{,\bar{x}} + c'_2 \bar{w}_{0,\bar{x}\bar{x}} + c'_3 \bar{\varphi}_{,\bar{x}\bar{x}}^+ + c'_4 \bar{\varphi}_{,\bar{x}\bar{x}}^- &= 0 \\ d'_1 \bar{u}_{0,\bar{x}} + d'_2 \bar{\psi}_{,\bar{x}} + d'_3 \bar{w}_{0,\bar{x}\bar{x}} + d'_4 \bar{\varphi}^+ + d'_5 \bar{\varphi}^- + d'_6 \bar{\varphi}_{,\bar{x}\bar{x}}^+ + d'_7 \bar{\varphi}_{,\bar{x}\bar{x}}^- &= d'_8 \\ e'_1 \bar{u}_{0,\bar{x}} + e'_2 \bar{\psi}_{,\bar{x}} + e'_3 \bar{w}_{0,\bar{x}\bar{x}} + e'_4 \bar{\varphi}^+ + e'_5 \bar{\varphi}^- + e'_6 \bar{\varphi}_{,\bar{x}\bar{x}}^+ + e'_7 \bar{\varphi}_{,\bar{x}\bar{x}}^- &= e'_8 \end{aligned} \quad (3.2)$$

where a'_i , b'_i , c'_i , d'_i , and e'_i are dimensionless constants.

In the present analysis, an analytical solution is obtained for the simply supported FGPM beam with the following boundary conditions as

$$\begin{aligned} \sigma_x = 0 &\rightarrow \bar{u}_{,\bar{x}} = \bar{\psi}_{,\bar{x}} = 0 & \bar{x} &= 0, 1 \\ \bar{w}_0 = 0 & & \bar{x} &= 0, 1 \\ \bar{\varphi} = 0 &\rightarrow \bar{\varphi}^+ = \bar{\varphi}^- = 0 & \bar{x} &= 0, 1 \end{aligned} \quad (3.3)$$

3.1. Finite Fourier transformation

To solve the system of equations (3.2), a finite Fourier transformation can be used as

$$\begin{aligned} \bar{u}_{0m} &= \int_0^1 \bar{u}_0(\bar{x}) \cos(m\pi\bar{x}) d\bar{x} & \bar{\psi}_m &= \int_0^1 \bar{\psi}_0(\bar{x}) \cos(m\pi\bar{x}) d\bar{x} \\ \bar{w}_{0m} &= \int_0^1 \bar{w}_0(\bar{x}) \sin(m\pi\bar{x}) d\bar{x} & \bar{\varphi}_m^+ &= \int_0^1 \bar{\varphi}_m^+(\bar{x}) \sin(m\pi\bar{x}) d\bar{x} \\ \bar{\varphi}_m^- &= \int_0^1 \bar{\varphi}_m^-(\bar{x}) \sin(m\pi\bar{x}) d\bar{x} \end{aligned} \quad (3.4)$$

Formulas for the inverse of transformation of Eqs. (3.4) are obtained by using a relationship from the theory of Fourier series

$$\begin{aligned}
 \bar{u}_0(\bar{x}) &= 2 \sum_m \bar{u}_{0m} \cos(m\pi\bar{x}) & \bar{\psi}(\bar{x}) &= 2 \sum_m \bar{\psi}_m \cos(m\pi\bar{x}) \\
 \bar{w}_0(\bar{x}) &= 2 \sum_m \bar{w}_{0m} \sin(m\pi\bar{x}) & \bar{\varphi}^+(\bar{x}) &= 2 \sum_m \bar{\varphi}_m^+ \sin(m\pi\bar{x}) \\
 \bar{\varphi}^-(\bar{x}) &= 2 \sum_m \bar{\varphi}_m^- \sin(m\pi\bar{x}) & m &= 1, 3, 5, \dots, \quad r = m\pi
 \end{aligned} \tag{3.5}$$

Solution (3.5) automatically satisfies boundary conditions (3.3). Applying transformation (3.4) to Eqs. (3.2) the following expressions are obtained

$$\begin{aligned}
 -r^2 a'_1 \bar{u}_{0m} - r^2 a'_2 \bar{\psi}_m + r a'_3 \bar{\varphi}_m^+ + r a'_4 \bar{\varphi}_m^- &= 0 \\
 b'_1 \bar{u}_{0m} + (b'_2 - r^2 b'_3) \bar{\psi}_m + r b'_4 \bar{w}_{0m} + r b'_5 \bar{\varphi}_m^+ + r b'_6 \bar{\varphi}_m^- &= 0 \\
 -r c'_1 \bar{\psi}_m - r^2 c'_2 \bar{w}_{0m} - r^2 c'_3 \bar{\varphi}_m^+ - r^2 c'_4 \bar{\varphi}_m^- &= \frac{2}{r} c'_5 \\
 -r d'_1 \bar{u}_{0m} - r d'_2 \bar{\psi}_m - r^2 d'_3 \bar{w}_{0m} + (d'_4 - r^2 d'_6) \bar{\varphi}_m^+ + (d'_5 - r^2 d'_7) \bar{\varphi}_m^- &= \frac{2}{r} d'_8 \\
 -r e'_1 \bar{u}_{0m} - r e'_2 \bar{\psi}_m - r^2 e'_3 \bar{w}_{0m} + (e'_4 - r^2 e'_6) \bar{\varphi}_m^+ + (e'_5 - r^2 e'_7) \bar{\varphi}_m^- &= \frac{2}{r} e'_8
 \end{aligned} \tag{3.6}$$

To find the m th Fourier components of $\bar{u}_{0m}, \bar{\psi}_m, \bar{w}_{0m}, \bar{\varphi}_m^+$ and $\bar{\varphi}_m^-$, the system of Eqs. (3.6) must be solved based on the choice of m . Using above Fourier components and applying into Eqs. (3.5), the series solution is determined.

3.2. Homotopy perturbation method

Various perturbation methods have been widely applied to solve linear and nonlinear problems. Unfortunately, the traditional perturbation techniques are based on the assumption that a small parameter must exist, which is too over-strict to find wide application (He, 2003). To illustrate the basic ideas of the new method, we consider the following differential equation

$$A(u) + f(r) = 0 \quad r \in \Omega \tag{3.7}$$

with boundary conditions

$$B\left(s, \frac{\partial s}{\partial q}\right) = 0 \quad r \in \Gamma \tag{3.8}$$

where A is a general differential operator, B is a boundary operator; $f(r)$ is a known analytic function, Γ is the boundary of the domain Ω (He, 1999;

Sajid *et al.*, 2006). The operator A can, generally speaking, be divided into two parts L and N , where L is linear, while N nonlinear, Eq. (3.7), therefore, can be rewritten as follows

$$L(s) + N(s) - f(r) = 0 \quad (3.9)$$

By the homotopy technique proposed by Liao (1995, 1997), we construct a homotopy of Eq. (3.7) $g(r, m): \Omega \times [0, 1] \rightarrow \Re$ which satisfies

$$J(g, m) = (1 - m)[L(g) - L(s_0)] + m[A(g) - f(r)] = 0 \quad m \in [0, 1], \quad r \in \Omega \quad (3.10)$$

or

$$J(g, m) = L(g) - L(s_0) + mL(s_0) + m[N(g) - f(r)] = 0 \quad (3.11)$$

where $m \in [0, 1]$ is an embedding parameter and s_0 is the initial approximation which satisfies the boundary conditions. Here the embedding parameter is introduced much more naturally, unaffected by artificial factors; further it can be considered as a small parameter for $0 \leq m \leq 1$.

So it is very natural to assume that the solution of Eq. (3.7) and Eq. (3.8) can be expressed as

$$g = g_0 + mg_1 + m^2g_2 + \dots \quad (3.12)$$

The approximate solution to Eq. (3.7), therefore, can be readily obtained

$$s = \lim_{g \rightarrow 1} g = g_0 + g_1 + g_2 + \dots \quad (3.13)$$

The convergence of the series of Eq. (3.13) has been proved in Takagi *et al.* (2003).

We construct a homotopy $\Omega \times [0, 1] \rightarrow \Re$ which satisfies

$$\begin{aligned} L_1(g) - L_1(s_0) + mL_1(s_0) + m[N_1(g) - f_1(r)] &= 0 \\ L_2(g) - L_2(s_0) + mL_2(s_0) + m[N_2(g) - f_2(r)] &= 0 \\ L_3(g) - L_3(s_0) + mL_3(s_0) + m[N_3(g) - f_3(r)] &= 0 \\ L_4(g) - L_4(s_0) + mL_4(s_0) + m[N_4(g) - f_4(r)] &= 0 \\ L_5(g) - L_5(s_0) + mL_5(s_0) + m[N_5(g) - f_5(r)] &= 0 \end{aligned} \quad (3.14)$$

where

$$\begin{aligned}
 L_1(g) &= \overline{u}_{0,\overline{xx}} & f_1(r) &= 0 \\
 N_1(g) &= \frac{a_2}{a_1}\overline{\psi}_{,\overline{xx}} + \frac{a_3}{a_1}\overline{\varphi}_{,\overline{x}}^+ + \frac{a_4}{a_1}\overline{\varphi}_{,\overline{x}}^- \\
 L_2(g) &= \overline{\psi}_{,\overline{xx}} & f_2(r) &= 0 \\
 N_2(g) &= \frac{b_1}{b_3}\overline{u}_{0,\overline{xx}} + \frac{b_2}{b_3}\overline{\psi}_{,\overline{x}} + \frac{b_4}{b_3}\overline{w}_{,\overline{xx}} + \frac{b_5}{b_3}\overline{\varphi}_{,\overline{x}}^+ + \frac{b_6}{b_3}\overline{\varphi}_{,\overline{x}}^- \\
 L_3(g) &= \overline{w}_{0,\overline{xx}} & f_3(r) &= 0 \\
 N_3(g) &= \frac{c_1}{c_2}\overline{\psi}_{,\overline{xx}} + \frac{c_3}{c_2}\overline{\varphi}_{,\overline{xx}}^+ + \frac{c_4}{c_2}\overline{\varphi}_{,\overline{xx}}^- \\
 L_4(g) &= \overline{\varphi}_{,\overline{xx}}^+ & f_4(r) &= \frac{d_8}{d_6} \\
 N_4(g) &= \frac{d_1}{d_6}\overline{u}_{0,\overline{x}} + \frac{d_2}{d_6}\overline{\psi}_{,\overline{x}} + \frac{d_2}{d_6}\overline{w}_{,\overline{xx}} + \frac{d_4}{d_6}\overline{\varphi}^+ + \frac{d_5}{d_6}\overline{\varphi}^- + \frac{d_7}{d_6}\overline{\varphi}_{,\overline{xx}}^- \\
 L_5(g) &= \overline{\varphi}_{,\overline{xx}}^- & f_5(r) &= \frac{e_1}{e_7} \\
 N_5(g) &= \frac{e_1}{e_7}\overline{u}_{0,\overline{x}} + \frac{e_2}{e_7}\overline{\psi}_{,\overline{x}} + \frac{e_3}{e_7}\overline{w}_{,\overline{xx}} + \frac{e_4}{e_7}\overline{\varphi}^+ + \frac{e_5}{e_7}\overline{\varphi}^- + \frac{e_6}{e_7}\overline{\varphi}_{,\overline{xx}}^+
 \end{aligned} \tag{3.15}$$

The initial approximation of Eq. (3.2) based on boundary conditions is assumed as

$$\begin{aligned}
 \overline{u}_0^0 &= \frac{1}{3}x^3 - \frac{1}{2}x^2 & \overline{\psi}^0 &= \frac{1}{3}x^3 - \frac{1}{2}x^2 \\
 \overline{w}_0^0 &= x^3 - x^2 & \overline{\varphi}^{+0} &= x^3 - x^2 \\
 \overline{\varphi}^{-0} &= x^3 - x^2
 \end{aligned} \tag{3.16}$$

Suppose the solution to Eq. (3.14) has the form

$$g = g_0 + mg_1 + m^2g_2 + \dots \tag{3.17}$$

Substituting Eq. (3.17) into (3.14), and equating the terms identically

$$\begin{aligned}
 m_{u_0}^0 : & \quad U_{0,\overline{xx}} = u_{0,\overline{xx}}^0 \\
 m_{u_0}^1 : & \quad U_{1,\overline{xx}} = -\left(u_{0,\overline{xx}}^0 + \frac{a_2}{a_1}\overline{\psi}_{,\overline{xx}}^0 + \frac{a_3}{a_1}\overline{\varphi}_{,\overline{x}}^{+0} + \frac{a_4}{a_1}\overline{\varphi}_{,\overline{x}}^{-0}\right) \\
 m_{u_0}^2 : & \quad U_{2,\overline{xx}} = -\left(\frac{a_2}{a_1}\overline{\psi}_{,\overline{xx}}^1 + \frac{a_3}{a_1}\overline{\varphi}_{,\overline{x}}^{+1} + \frac{a_4}{a_1}\overline{\varphi}_{,\overline{x}}^{-1}\right) \\
 m_{u_0}^3 : & \quad U_{3,\overline{xx}} = -\left(\frac{a_2}{a_1}\overline{\psi}_{,\overline{xx}}^2 + \frac{a_3}{a_1}\overline{\varphi}_{,\overline{x}}^{+2} + \frac{a_4}{a_1}\overline{\varphi}_{,\overline{x}}^{-2}\right) \\
 m_{\psi}^0 : & \quad \Psi_{0,\overline{xx}} = \overline{\psi}_{,\overline{xx}}^0 \\
 m_{\psi}^1 : & \quad \Psi_{1,\overline{xx}} = -\left(\overline{\psi}_{,\overline{xx}}^0 + \frac{b_1}{b_3}\overline{u}_{,\overline{xx}}^0 + \frac{b_2}{b_3}\overline{\psi}_{,\overline{x}}^0 + \frac{b_4}{b_3}\overline{w}_{,\overline{x}}^0 + \frac{b_5}{b_3}\overline{\varphi}_{,\overline{x}}^{+0} + \frac{b_6}{b_3}\overline{\varphi}_{,\overline{x}}^{-0}\right)
 \end{aligned}$$

$$\begin{aligned}
m_{\psi}^2 : \quad \Psi_{2,\bar{x}\bar{x}} &= -\left(\frac{b_1}{b_3}\bar{u}_{,\bar{x}\bar{x}}^1 + \frac{b_2}{b_3}\bar{\psi}^1 + \frac{b_4}{b_3}\bar{w}_{,\bar{x}}^1 + \frac{b_5}{b_3}\bar{\varphi}_{,\bar{x}}^{+1} + \frac{b_6}{b_3}\bar{\varphi}_{,\bar{x}}^{-1}\right) \\
m_{\psi}^3 : \quad \Psi_{3,\bar{x}\bar{x}} &= -\left(\frac{b_1}{b_3}\bar{u}_{,\bar{x}\bar{x}}^2 + \frac{b_2}{b_3}\bar{\psi}^2 + \frac{b_4}{b_3}\bar{w}_{,\bar{x}}^2 + \frac{b_5}{b_3}\bar{\varphi}_{,\bar{x}}^{+2} + \frac{b_6}{b_3}\bar{\varphi}_{,\bar{x}}^{-2}\right) \\
m_{w_0}^0 : \quad W_{0,\bar{x}\bar{x}} &= w_{0,\bar{x}\bar{x}}^0 \\
m_{w_0}^1 : \quad W_{1,\bar{x}\bar{x}} &= -\left(w_{0,\bar{x}\bar{x}}^0 + \frac{c_1}{c_2}\bar{\psi}_{,\bar{x}}^0 + \frac{c_3}{c_2}\bar{\varphi}_{,\bar{x}\bar{x}}^{+0} + \frac{c_4}{c_2}\bar{\varphi}_{,\bar{x}\bar{x}}^{-0}\right) \\
m_{w_0}^2 : \quad W_{2,\bar{x}\bar{x}} &= -\left(\frac{c_1}{c_2}\bar{\psi}_{,\bar{x}}^1 + \frac{c_3}{c_2}\bar{\varphi}_{,\bar{x}\bar{x}}^{+1} + \frac{c_4}{c_2}\bar{\varphi}_{,\bar{x}\bar{x}}^{-1}\right) \\
m_{w_0}^3 : \quad W_{3,\bar{x}\bar{x}} &= -\left(\frac{c_1}{c_2}\bar{\psi}_{,\bar{x}}^2 + \frac{c_3}{c_2}\bar{\varphi}_{,\bar{x}\bar{x}}^{+2} + \frac{c_4}{c_2}\bar{\varphi}_{,\bar{x}\bar{x}}^{-2}\right) \\
m_{\varphi^+}^0 : \quad \Phi_{0,\bar{x}\bar{x}}^+ &= \varphi_{,\bar{x}\bar{x}}^{+0} \\
m_{\varphi^+}^1 : \quad \Phi_{1,\bar{x}\bar{x}}^+ &= -\left(\varphi_{,\bar{x}\bar{x}}^{+0} + \frac{d_1}{d_6}\bar{u}_{,\bar{x}}^0 + \frac{d_2}{d_6}\bar{\psi}_{,\bar{x}}^0 + \frac{d_3}{d_6}\bar{w}_{,\bar{x}\bar{x}}^0 + \frac{d_4}{d_6}\bar{\varphi}^{+0} + \frac{d_5}{d_6}\bar{\varphi}^{-0} + \right. \\
&\quad \left. + \frac{d_7}{d_6}\bar{\varphi}_{,\bar{x}\bar{x}}^{-0}\right) \\
m_{\varphi^+}^2 : \quad \Phi_{2,\bar{x}\bar{x}}^+ &= -\left(\frac{d_1}{d_6}\bar{u}_{,\bar{x}}^1 + \frac{d_2}{d_6}\bar{\psi}_{,\bar{x}}^1 + \frac{d_3}{d_6}\bar{w}_{,\bar{x}\bar{x}}^1 + \frac{d_4}{d_6}\bar{\varphi}^{+1} + \frac{d_5}{d_6}\bar{\varphi}^{-1} + \frac{d_7}{d_6}\bar{\varphi}_{,\bar{x}\bar{x}}^{-1}\right) \\
m_{\varphi^+}^3 : \quad \Phi_{3,\bar{x}\bar{x}}^+ &= -\left(\frac{d_1}{d_6}\bar{u}_{,\bar{x}}^2 + \frac{d_2}{d_6}\bar{\psi}_{,\bar{x}}^2 + \frac{d_3}{d_6}\bar{w}_{,\bar{x}\bar{x}}^2 + \frac{d_4}{d_6}\bar{\varphi}^{+2} + \frac{d_5}{d_6}\bar{\varphi}^{-2} + \frac{d_7}{d_6}\bar{\varphi}_{,\bar{x}\bar{x}}^{-2}\right) \\
m_{\varphi^-}^0 : \quad \Phi_{0,\bar{x}\bar{x}}^- &= \varphi_{,\bar{x}\bar{x}}^{-0} \\
m_{\varphi^-}^1 : \quad \Phi_{1,\bar{x}\bar{x}}^- &= -\left(\varphi_{,\bar{x}\bar{x}}^{-0} + \frac{e_1}{e_7}\bar{u}_{,\bar{x}}^0 + \frac{e_2}{e_7}\bar{\psi}_{,\bar{x}}^0 + \frac{e_3}{e_7}\bar{w}_{,\bar{x}\bar{x}}^0 + \frac{e_4}{e_7}\bar{\varphi}^{+0} + \frac{e_5}{e_7}\bar{\varphi}^{-0} + \right. \\
&\quad \left. + \frac{e_6}{e_7}\bar{\varphi}_{,\bar{x}\bar{x}}^{+0}\right) \\
m_{\varphi^-}^2 : \quad \Phi_{2,\bar{x}\bar{x}}^- &= -\left(\frac{e_1}{e_7}\bar{u}_{,\bar{x}}^1 + \frac{e_2}{e_7}\bar{\psi}_{,\bar{x}}^1 + \frac{e_3}{e_7}\bar{w}_{,\bar{x}\bar{x}}^1 + \frac{e_4}{e_7}\bar{\varphi}^{+1} + \frac{e_5}{e_7}\bar{\varphi}^{-1} + \frac{e_6}{e_7}\bar{\varphi}_{,\bar{x}\bar{x}}^{+1}\right) \\
m_{\varphi^-}^3 : \quad \Phi_{3,\bar{x}\bar{x}}^- &= -\left(\frac{e_1}{e_7}\bar{u}_{,\bar{x}}^2 + \frac{e_2}{e_7}\bar{\psi}_{,\bar{x}}^2 + \frac{e_3}{e_7}\bar{w}_{,\bar{x}\bar{x}}^2 + \frac{e_4}{e_7}\bar{\varphi}^{+2} + \frac{e_5}{e_7}\bar{\varphi}^{-2} + \frac{e_6}{e_7}\bar{\varphi}_{,\bar{x}\bar{x}}^{+2}\right)
\end{aligned} \tag{3.18}$$

Consequently, solving the above equations, the components of the homotopy perturbation solution for the system of Eqs. (3.2) are derived.

4. Results

The numerical results are presented using the theory of Fourier series in this paper. The present study considers functionally graded materials composed of two piezo-electric constitutive materials. The bottom surface of the FGPM

beam is Platinum whereas the top surface of the beam is PZT-4-rich. The material properties of PZT-4 and Platinum are shown in Table 1.

Table 1. Material properties of PZT-4 and platinum

PZT-4	Platinum
$\widehat{E} = 74 \text{ GPa}$, $K = 9 \text{ W/(mK)}$, $\alpha = 4.4 \cdot 10^{-6} \text{ 1/K}$, $e_{31} = -0.9 \text{ C/m}^2$, $e_{15} = 4.6 \text{ C/m}^2$, $\eta_{11} = 8.26 \cdot 10^{-11} \text{ N/m}^2$, $\eta_{33} = 9.03 \cdot 10^{-11} \text{ N/m}^2$, $p_3 = 3 \cdot 10^{-6} \text{ C/(Km}^2)$	$\widehat{E} = 168 \text{ GPa}$, $K = 77.8 \text{ W/(mK)}$, $\alpha = 9 \cdot 10^{-6} \text{ 1/K}$, $e_{31} = 0$, $e_{15} = 0 \text{ C/m}^2$, $\eta_{11} = 0 \text{ N/m}^2$, $\eta_{33} = 0 \text{ N/m}^2$, $p_3 = 0 \text{ C/(Km}^2)$

The FGPM beam of length of 0.2 m and height 0.0025 m with simply supported conditions is assumed. The FGPM beam is studied under a thermal gradient through its thickness direction. The temperature of the top PZT-4-rich surface is fixed at 400 K and that of bottom Platinum surface is kept constant at 300 K. It is assumed that the reference temperature is $T_0 = 295 \text{ K}$. The temperature field through the thickness of the beam is shown in Fig. 2.

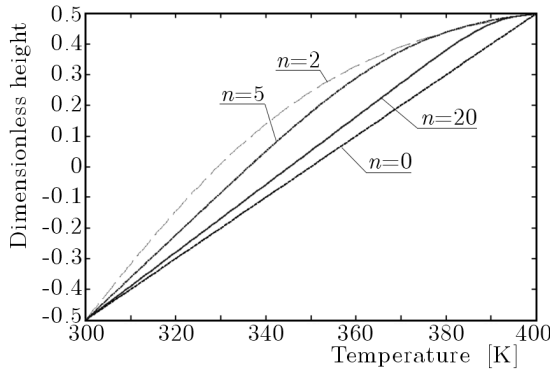


Fig. 2. Distribution of temperature through dimensionless height of the FGPM beam

According to Eqs. (3.16) and (3.18), the first few components of the homotopy perturbation solution for the system of Eqs. (3.2), for $n = 0$, are derived as

$$\begin{aligned}
 W_0 &= x^3 - x^2 \\
 W_1 &= -0.28571x^4 - 0.812x^3 + 0.833x^2 \\
 W_2 &= 0.001241x^6 - 0.0148x^5 + 0.2742x^4 - 0.212x^3 + 0.1971x^2 \\
 W_3 &= 0.000051x^8 + 0.000034x^7 - 0.001156x^6 + 0.01791x^5 + 0.008331x^4 + \\
 &\quad + 0.0189x^3 - 0.02493x^2
 \end{aligned}
 \tag{4.1}$$

Thus we have a fourth order of approximation for the dimensionless lateral deflection and the dimensionless electric potentials of Eqs. (3.2)

$$\begin{aligned} W &= W_0 + W_1 + W_2 + W_3 + \dots \\ \Phi &= \Phi_0^+ + \Phi_1^+ + \Phi_2^+ + \Phi_3^+ + \dots \\ \Phi_0 &= \Phi_0^- + \Phi_1^- + \Phi_2^- + \Phi_3^- + \dots \end{aligned} \quad (4.2)$$

And so on, in this manner the rest of components of the homotopy perturbation solution for the system of Eqs. (3.2) can be obtained for $n = 0$. The solution is given by

$$\begin{aligned} W &= 5.1 \cdot 10^{-5}x^8 + 3.4 \cdot 10^{-5}x^7 - 8.5 \cdot 10^{-5}x^6 + 3.111 \cdot 10^{-3}x^5 + \\ &- 3.179 \cdot 10^{-3}x^4 - 5.1 \cdot 10^{-3}x^3 + 5.168 \cdot 10^{-3}x^2 \end{aligned} \quad (4.3)$$

Table 2 is presented to show the effect of the power law index of the functionally graded piezoelectric beam for distribution of dimensionless deflection through the dimensionless length. The results obtained by the homotopy perturbation method are compared with the finite Fourier transformation for different power law indexes. Table 2 shows that with the increase of n , when the beam constituent materials change from the PZT-4-rich to the Platinum-rich, the midpoint deflection of the FGPM beam decreases accordingly. It is seen that for larger values of n , the deflection of the beam is changed and decreased evidently. The top and bottom surfaces variation of dimensionless electric potential through the dimensionless length of the FGPM beam caused by thermal load for different power law indexes are shown in Figs. 3-7. The figures show that for most Platinum-rich FGPM beam, (higher values of n), the electric potential distribution decreases in value due to less piezoelectric constants. Good agreements are observed between the homotopy perturbation method and the finite Fourier transformation.

Table 2. Maximum deflection in simply-supported FGPM beam

n	Finite Fourier method	HPM method	Error
0	$5.762 \cdot 10^{-4}$	$5.521 \cdot 10^{-4}$	4.18%
2	$3.462 \cdot 10^{-5}$	$3.31 \cdot 10^{-5}$	4.3%
5	$1.01 \cdot 10^{-6}$	$0.96 \cdot 10^{-6}$	4.98%
10	$0.453 \cdot 10^{-6}$	$0.432 \cdot 10^{-6}$	4.63%

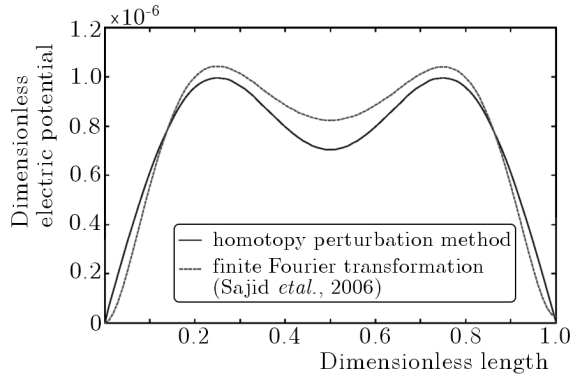


Fig. 3. Top surface variation of dimensionless electric potential through dimensionless length of the FGPM beam caused by thermal load for $n = 2$

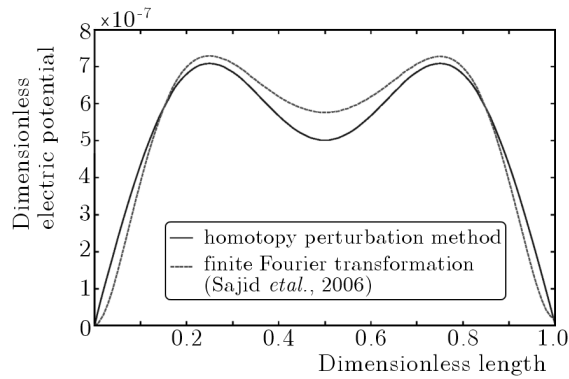


Fig. 4. Top surface variation of dimensionless electric potential through dimensionless length of the FGPM beam caused by thermal load for $n = 5$

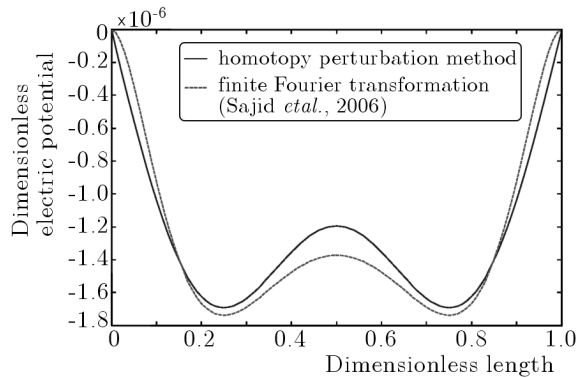


Fig. 5. Bottom surface variation of dimensionless electric potential through dimensionless length of the FGPM beam caused by thermal load for $n = 0$

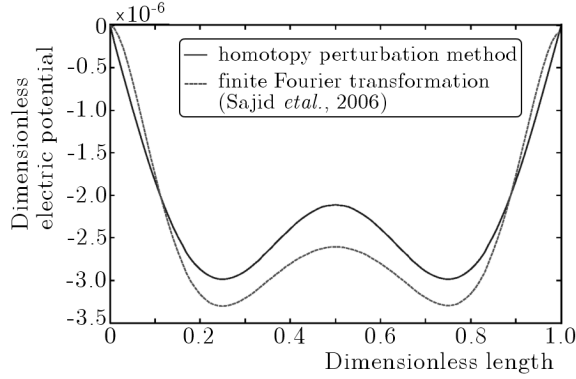


Fig. 6. Bottom surface variation of dimensionless electric potential through dimensionless length of the FGPM beam caused by thermal load for $n = 2$

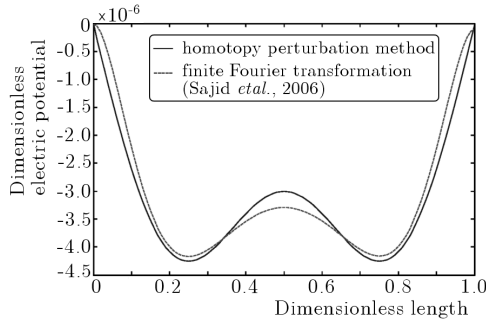


Fig. 7. Bottom surface variation of dimensionless electric potential through dimensionless length of the FGPM beam caused by thermal load for $n = 5$

5. Conclusions

In the present paper, the static analysis of an FGPM beam based on the first-order shear deformation theory under thermal load is investigated. The beam is subjected to constant surface temperatures on the upper and lower surfaces. Boundary conditions of the beam are taken to be simply supported at the ends of the beam. To solve the problem, the numerical homotopy perturbation method is used. Moreover, the results are compared with the finite Fourier transformation for different power law indexes. They show that for larger values of power law indexes which provide less PZT-4 rich FGPM, the lateral deflection of the FGPM beam decreases constantly due to the applied thermal load. By increasing the metal share in the FGPM beam, the maximum value

of electric potential decreases on the top and bottom beam surfaces. Moreover, the obtained results show the accuracy of this approach and reveal that the proposed homotopy perturbation method is very effective and simple to the problem like this. It can be predicted that HPM is a suitable method for other FGPM problems in which exact solutions are not easily achieved.

Appendix A

$$\begin{aligned}
 A'_1 &= \int \widehat{E}(z) dz & A'_2 &= \int -z\widehat{E}(z) dz \\
 A'_3 &= \int \frac{e_{31}(z)}{h} dz & A'_4 &= \int -\frac{e_{31}(z)}{h} dz \\
 B'_1 &= \int -z\widehat{E}(z) dz & B'_2 &= \int \widehat{G}(z) dz \\
 B'_3 &= \int z^2\widehat{E}(z) dz & B'_4 &= \int -\widehat{G}(z) dz \\
 B'_5 &= \int \left[-\frac{ze_{31}(z)}{h} - \left(\frac{z}{h} + \frac{1}{2}\right)e_{15}(z) \right] dz \\
 B'_6 &= \int \left[\frac{ze_{31}(z)}{h} - \left(\frac{z}{h} - \frac{1}{2}\right)e_{15}(z) \right] dz \\
 C'_1 &= \int -\widehat{G}(z) dz & C'_2 &= \int \widehat{G}(z) dz \\
 C'_3 &= \int \left(\frac{z}{h} + \frac{1}{2}\right)e_{15}(z) dz & C'_4 &= \int \left(-\frac{z}{h} + \frac{1}{2}\right)e_{15}(z) dz \\
 D'_1 &= \int \frac{e_{31}(z)}{h} dz & D'_2 &= \int \left[-\frac{ze_{31}(z)}{h} - \left(\frac{z}{h} + \frac{1}{2}\right)e_{15}(z) \right] dz \\
 D'_3 &= \int \left(\frac{z}{h} + \frac{1}{2}\right)e_{15}(z) dz & D'_4 &= \int -\frac{\eta_{33}(z)}{h^2} dz \\
 D'_5 &= \int \frac{\eta_{33}(z)}{h^2} dz & D'_6 &= \int -\eta_{11}(z) \left(\frac{z^2}{h^2} + \frac{z}{h} + \frac{1}{4}\right) dz \\
 D'_7 &= \int \eta_{11}(z) \left(\frac{z^2}{h^2} - \frac{1}{4}\right) dz & D'_8 &= \int -\frac{p_3(z)\theta(z)}{h} dz \\
 E'_1 &= \int -\frac{e_{31}(z)}{h} dz & E'_2 &= \int \left[\frac{ze_{31}(z)}{h} + \left(\frac{z}{h} - \frac{1}{2}\right)e_{15}(z) \right] dz \\
 E'_3 &= \int -\left(\frac{z}{h} - \frac{1}{2}\right)e_{15}(z) dz & E'_4 &= \int \frac{\eta_{33}(z)}{h^2} dz \\
 E'_5 &= \int -\frac{\eta_{33}(z)}{h^2} dz & E'_6 &= \int \eta_{11}(z) \left(\frac{z^2}{h^2} - \frac{1}{4}\right) dz \\
 E'_7 &= \int -\eta_{11}(z) \left(\frac{z}{h} - \frac{1}{2}\right)^2 dz & E'_8 &= \int \frac{p_3(z)\theta(z)}{h} dz
 \end{aligned}$$

References

1. CHEN W.Q., BIAN Z.G., LV C.F., DING H.J., 2004, 3D free vibration analysis of a functionally graded piezoelectric hollow cylinder filled with compressible fluid, *International Journal of Solids and Structures*, **41**, 947-964
2. TAKAGI K., LI J.F., YOKOYAMA S., WATANABE R., 2003, Fabrication and evaluation of PZT/Pt piezoelectric composites and functionally graded actuators, *Journal of the European Ceramic Society*, **23**, 1577-1586
3. WU X.H., CHEN C.Q., SHEN Y.P., TIAN X.G., 2002, A high order theory for functionally graded piezoelectric shells, *International Journal of Solids and Structures*, **39**, 5325-5344
4. JIN D.R., MENG Z.Y., 2003, Functionally graded PZT/ZnO piezoelectric composites, *Journal of Material Science Letters*, **22**, 971-974
5. PIN L., LEE H.P., LU C., 2006, Exact solutions for simply supported functionally graded piezoelectric laminates by Stroh-like formalism, *Composite Structures*, **72**, 352-363
6. LIAO S.J., 1995, An approximate solution technique not depending on small parameters: a special example, *Journal of Nonlinear Mechanics*, **30**, 371-380
7. LIAO S.J., 1997, Boundary element method for general nonlinear differential operators, *Engineering Analysis with Boundary Elements*, **20**, 91-99
8. LANHE W., HONGIUN W., DAOBIN W., 2007, Nonlinear dynamic stability analysis of FGM plates by the moving least squares differential quadrature method, *Composite Structures*, **77**, 383-394
9. WANG B.L., NODA N., 2001, Design of a smart functionally graded thermopiezoelectric composite structure, *Smart Materials and Structures*, **10**, 189-193
10. KAPURIA S., AHMED A., DUMIR P.C., 2004, Coupled consistent third-order theory for hybrid piezoelectric beams under thermal load, *Journal of Thermal Stress*, **27**, 405-424
11. TRINDADE M.A., BENJEDDOU A., 2006, On higher-order modelling of smart beams with embedded shear-mode piezoceramic actuators and sensors, *Mechanics of Advanced Materials and Structures*, **13**, 357-369
12. HE J.H., 2003, Homotopy perturbation method: a new nonlinear analytical technique computer methods, *Applied Mechanics and Engineering*, **135**, 73-79
13. HE J.H., 1999, Homotopy perturbation technique, *Computer Methods in Applied Mechanics and Engineering*, **178**, 257-262
14. SAJID M., HAYAT T., ASGHAR S., 2006, On the analytic solution of steady flow of a fourth grade fluid, *Physics Letter A*, **355**, 18-24

Porównanie rezultatów analizy statycznej belki FGPM otrzymanych metodą HPM i za pomocą skończonej transformacji Fouriera

Streszczenie

Zjawiska liniowe i nieliniowe odgrywają ważną rolę w dziedzinie matematyki stosowanej, fizyki, a także zagadnieniach inżynierskich, w których dowolny parametr może ulegać zmianie pod wpływem różnych czynników. W ostatnich latach perturbacyjna metoda homotopii (HPM) ulegała ciągłemu rozwojowi i znalazła zastosowanie w rozwiązywaniu różnorodnych liniowych i nieliniowych zadań. W tej pracy zaprezentowano wyniki analizy statycznej belki wykonanej z gradientowego materiału zawierającego frakcję piezoelektryczną i obciążonej termicznie otrzymanych przy pomocy teorii odkształceń postaciowych pierwszego rzędu. Belka z materiału funkcjonalnego (FGPM) ma strukturę gradientową, tj. posiada właściwości materiałowe zmienne w sposób ciągły wzdłuż grubości tej belki, zgodnie z założonym rozkładem wykładniczym zawartości aktywnej frakcji piezoelektryka w całym materiale. Założono, że potencjał elektryczny ma rozkład liniowy wzdłuż grubości belki. Różniczkowe równania ruchu układu otrzymano, używając wyrażenia na energię potencjalną i stosując zasadę Hamiltona. Do ich rozwiązania zaproponowano dwie metody: perturbacyjną homotopii i analityczną w drodze skończonej transformacji Fouriera. W metodzie homotopii zasugerowano odpowiedni algorytm rozwiązywania układu równań różniczkowych. Wyniki przedstawiono dla różnych rozkładów aktywnej frakcji piezoelektrycznej przy utrzymaniu jednorodnego gradientu temperatury. Wyniki porównano z rozwiązaniem analitycznym otrzymanym za pomocą skończonej transformacji Fouriera dla warunków brzegowych belki odpowiadających swobodnemu podparciu.

Manuscript received April 6, 2009; accepted for print July 2, 2009